Atmosphere and dose effects on the SHI irradiation of atactic polystyrene

Muriel Ferry, Manon Cornaton, Delphine Durand, Stéphane Esnouf, Caroline Aymes-Chodur, Yvette Ngono-Ravache

Atmosphere and dose effects on the SHI irradiation of atactic polystyrene

Muriel Ferry[1], Manon Cornaton[1], Delphine Durand[1], Stéphane Esnouf[1], Caroline Aymes-Chodur[2] and Yvette Ngono[3]

[1] *Université Paris-Saclay, CEA, Service de Physico-Chimie, 91191, Gif-sur-Yvette, France*

[2] *Université Paris-Saclay, ICMMO / SM2ViE, CNRS UMR 8182, F-91405, Orsay Cedex, France*

[3] *CIMAP (CEA/CNRS/ENSICaen/UCN), Caen, France*

Abstract

This article deals with Swift Heavy Ion (SHI) irradiation of atactic polystyrene at different doses, up to about 10 MGy, under an inert and oxidative atmosphere. The effect of the irradiation is analyzed using various tools such as high-resolution gas mass spectrometry, gel fraction, size exclusion chromatography, and Fourier Transform InfraRed spectroscopy. Previous research has shown that under SHI and in conditions of homogenous oxidation, two kinds of defects can be identified: those commonly observed under an oxidative atmosphere with low linear energy transfer irradiations (hydroperoxides and carbonyl bonds, for instance), and those evidenced under inert atmosphere (C=C bonds...). These latter defects are assigned to the heterogeneous structure of energy deposition with ion beams because of ion tracks' high ionization and excitation density. Polystyrene (PS) is known to be very radiation-resistant under inert atmosphere. Although degradation is increased under oxidative atmosphere, the oxidation remains very low compared to the one observed in polyethylene, even at doses as high as 10 MGy. The global low oxidation of PS under oxidative atmosphere is explained, as under inert atmosphere, by the presence of aromatic rings that confers efficient radiation resistence to the polymer.

Keywords

Polystyrene; α-emitters simulation; Gas radiation chemical yields; Atmosphere of irradiation effect; Dose effect; Heterogeneous energy deposition

Highlights

- α-emitters irradiation has been simulated using by using Swift Heavy Ion beams
- Effect of oxygen on the irradiation of polystyrene has been evaluated
- Effect of dose of the irradiated polystyrene has been studied
- H_2 and CO_2 release evolution has been analysed to understand ageing

Introduction

Polymers are materials widely employed in the nuclear power industry as electric cables insulators (Hettal et al., 2021; Xu et al., 2021), seals (Skidmore, 2012), glove-boxes gloves (Fromentin et al., 2017), etc. Because these polymers have been in contact with non-natural radioactivity, they are discarded as nuclear waste at the end of their lifetime; some of them are discarded specifically into Long-Lived Intermediate Level waste (LL-ILW) packages. In France, it is foreseen to place this kind of waste in a deep geological repository, for which a reversibility period of 100 years has to be taken into account (during the first 100 years, all waste packages need to be accessible and removed from the repository in the case that a better solution for the waste treatment is found). Researchers must carefully understand the polymer's behavior when in contact with the different types of radionuclides as a function of the emitter (*e.g*., the irradiation nature), the atmosphere (*e.g*., inert or oxidative), and the waste package age (*e.g*., the dose).

Numerous publications have studied the polymer's behavior in LL-ILW packages. During the last twelve years, a collaborative program between Orano and the CEA has investigated different irradiation conditions and different polymers (Boughattas et al., 2016; Ferry et al., 2021a; Ferry et al., 2016b; Furtak-Wrona et al., 2019; Ngono-Ravache et al., 2015). Recent efforts have focused on developing tools allowing Swift Heavy Ions (SHI) irradiations: Ferry *et al.* (Ferry et al., 2021b) for example, obtained results on polyethylene, polystyrene, and two types of polyurethanes, which were compared to the literature for irradiations under inert atmosphere (Chang and LaVerne, 2000). Results were then compared with those obtained and later on under oxidative atmosphere. The most sensitive material to Linear Energy Transfer (LET) was determined to be polystyrene. This polymer is not strictly speaking used in the nuclear industry, but due to its dependence on stopping power, it seemed important to include it in studies on the aging of polymers in nuclear waste packages.

Under an inert atmosphere or vacuum, crosslinking is the predominant mechanism in PS irradiated with SHI (Bouffard et al., 1997; Klaumünzer et al., 1996; Puglisi et al., 1986). According to Puglisi *et al.* (Puglisi et al., 1986), the solubility decrease associated to interchains crosslinking presents a similar evolution to the decrease of benzene ring quantity: these authors associate this to a crosslinking mechanism happening through cyclohexadiene bridges without dihydrogen emission. On the contrary, Klaumünzer *et al.* (Klaumünzer et al., 1996) remarked that crosslinking radiation chemical yields evolved very similarly to the hydrogen radiation chemical yields obtained by Lewis and Lee (Lewis and Lee, 1993). They conclude that the same mechanism would be at the origin of these two defects' formation, which would discard the one proposed by Puglisi *et al.* (Puglisi et al., 1986). From a molecular level, researchers have offered evidence of the

formation of disubstituted aromatic rings, double bonds, and benzene; the latter two defects follow a similar evolution as a function of the electronic stopping power (Balanzat et al., 1996; Dole, 1972; Ferry et al., 2008).

Ion irradiations under an inert atmosphere give the first insight into polystyrene's aging and its sensitivity towards stopping power. Nonetheless, parameters such as the irradiation atmosphere and the dose *(e.g.,* defects accumulation) highly modify the aging mechanisms. To our knowledge, polystyrene irradiation under an oxidative atmosphere has never been studied using SHI irradiations and has only barely been studied under four types of low LET irradiation: photo-oxidation (Geuskens et al., 1978a; Geuskens et al., 1978b; Mailhot and Gardette, 1992), in-pile irradiation or 1 MeV electrons beam (Alexander and Toms, 1956), γ-rays (Bowmer et al., 1979), or low energy ion irradiation (Choi et al., 1999). Enhanced degradation of polystyrene was observed in each case, whether by evaluating scissions and crosslinking, new bond formation, wettability, or mechanical properties.

This work gives further insights into oxygen influence at different doses on the SHI irradiation of atactic polystyrene (APS). To our knowledge, combining oxygen surrounding atmosphere and SHI irradiation on polystyrene has never been studied.

1. Experimental section

1.1. Material

The atactic polystyrene chosen for this study is pure APS Goodfellow reference ST311025. Its nominal thickness is given at 25 µm but was determined to be 28 µm by weighing, considering ρ = 1.05 $g.mol^{-1}$.

1.2. Swift Heavy Ions irradiation

As indicated in previous articles, a two-step irradiation procedure is necessary when considering gas emission radiation chemical yields at high doses (Ferry et al., 2021a; Ferry et al., 2016b; Fromentin et al., 2017). This procedure avoids total consumption of oxygen when using a closed container or H_2 back reactions if its concentration becomes too high.

Both irradiation steps were performed at the Grand Accélérateur National d'Ions Lourds (GANIL, Caen, France). Ion energies were high enough to ensure a relatively constant LET through the samples' thickness. During both steps, samples were irradiated as a stack of thin films, and the

number of films superimposed was chosen to ensure a relative variation of the LET, below 25%, from the stack entrance to its exit.

The first irradiation step was performed on the Medium Energy Line facility (SME), using a 7.1 MeV/A ^{16}O beam. Irradiations were performed in a large volume irradiation chamber under 1 bar of nitrogen or 1 bar of oxygen. After the first irradiation step, polymers were retrieved and stored under an inert atmosphere and in a dark place to prevent further aging as much as possible.

The second irradiation step was performed in closed glass ampoules to collect gases. This study used two kinds of glass ampoules: sealed ampoules and ampoules equipped with a valve. These ampoules were chosen because they are activated during the SHI irradiations, and their deactivation takes at least one month. Sealed ampoules at about 700 mbar of helium are used when irradiations are performed under an inert atmosphere with no difficulty. However, the post-oxidation effect must be avoided after irradiation under an oxidative atmosphere. In these conditions, glass ampoules equipped with a valve are employed and filled at around 700 mbar of reconstituted air (20.00 % O_2, 77.99 % N_2, 2.01 % Kr). Krypton is used as a tracer to determine the final pressure. The valve is used to collect the gas sample right at the end of the irradiation, eliminating the post-oxidation risks in our analyses.

After preparation, glass ampoules were irradiated on the High Energy Line facility (HE) using an 87.5 MeV/A ^{36}Ar beam. The use of high energy ^{36}Ar beam for the second step is justified by the need: *i*) to go through the ampoule glass walls without drastically reducing the energy of the beam before reaching the samples placed in these ampoules and *ii*) to limit the LET variation through the film stack below 25 %, as explained above.

Homogeneous irradiation is ensured by an x,y-scanned beam (typically 25 cm^2 for the SME facility and 36 cm^2 for the HE facility). The energy loss is calculated with SRIM based on the TRIM code (Ziegler et al., 2010). Irradiation conditions are gathered in Table 1. Fluxes are chosen to limit the power deposition on samples to 0.5 $mW.cm^{-2}$, avoiding significant sample heating. Statistical errors for a given sample and a single beam are negligible, at most a few %. The systematic errors are higher and are mainly due to sample thickness and dose estimation (less than 10% of material composition changes). The total error on dose is estimated at 10%.

Table 1. Irradiation conditions, dose rates, and doses received by the different pre-aged samples using ^{16}O ions irradiations (pre-aging step) and ^{36}Ar ions irradiations (second step) at room temperature. E_i is the energy of the projectiles at the film stack entrance; LET is the mean value of the LET in the sample. Two ampoules were prepared and irradiated for the second step irradiation, the first one at a dose of around 0.5 MGy and the second one at about 1 MGy.

Initial dose (MGy)	**Atmosphere**	**E_i (MeV.A^{-1})**	**LET (MeV.mg^{-1}.cm^{-2})**	**Flux (10^8 cm^{-2}.s^{-1})**	**Fluence (10^{12} cm^{-2})**	**Mean dose rate (MGy.h^{-1})**	**Mean dose (MGy)**
First irradiation step (SME ^{16}O ions irradiation)							
0	Oxygen	3.37	6.83	2.40	1.83	0.947	2.00
0					3.66		4.00
0					9.14		10.00
0	Nitrogen	3.56	6.56	2.68	1.90	1.057	2.08
0					3.81		4.17
0					9.52		10.41
Second irradiation step (He ^{36}Ar ions irradiation)							
0	Air	89	2.46	3.26	1.26 ; 2.51	0.463	0.47 ; 0.94
2.00					1.14 ; 2.27		0.44 ; 0.91
4.00					1.26 ; 2.51		0.50 ; 1.07
10.00					1.14 ; 2.40		0.46 ; 0.95
0	Helium	89	2.50	3.24	1.26 ; 2.51	0.467	0.47 ; 0.94
2.08					1.26 ; 2.27		0.52 ; 0.95
4.17					1.26 ; 2.51		0.51 ; 1.02
10.41					1.26 ; 2.27		0.51 ; 0.94

For irradiations performed under an oxidative atmosphere, the critical thickness of oxidation, below which oxidation is homogenous, is calculated thanks to Gillen and Clough's equation (Gillen and Clough, 1991). This critical thickness is always higher than the thickness of the samples of this study, which implies that in both the first step and the second step of the irradiation protocol, oxidation is not limited by O_2 diffusion, regarless of the dose.

1.3. Characterization

1.3.1. Gas quantification

Radiolysis gases produced in each glass ampoule were analyzed using a Thermo Fischer Scientific MAT-271 spectrometer equipped with different detectors (Faraday cups but also electron multiplier). A previous article (Ferry et al., 2014) has described this experimental setup in detail. The use of the gas mass spectrometer justifies the choice of helium when irradiations are performed under an inert atmosphere: using helium instead of nitrogen allows for avoiding interferences with carbon oxide fragments at m/z 28.

Radiation chemical yield $G(Y)$ of a gas Y was determined using Equation 1, assuming that the ideal gas law is respected:

$$G(Y) = \frac{P_f \cdot \%_{vol} \cdot V_{free}}{R \cdot T \cdot D \cdot m}, \qquad \text{Equation 1}$$

where G is in units of mol.J^{-1}, P_f is the total pressure in the glass ampoule at the end of the irradiation in Pa, $\%_{vol}$ is the gas volume fraction, V_{free} is the free volume in the glass ampoule in m^3, R is the gas constant, T is the sample's temperature under irradiation in K, D is the dose deposited during the irradiation in Gy, and m is the mass of the irradiated sample in kg.

1.3.1. Soluble fraction

Pristine and irradiated polymers were dissolved in tetrahydrofuran (THF) at room temperature for a few hours under stirring. Most of the solution of the solubilized polymer was then pipetted and transferred into vials that were left under a laboratory fume hood for 48 hours for solvent evaporation before weighing.

The soluble fraction is determined using the equation given in Equation 2:

$$S = \frac{m_0 - m_s}{m_0} \cdot 100, \qquad \text{Equation 2}$$

where S is the soluble fraction (in %), m_0 is the initial polymer mass (in g), and m_s (in g) is the polymer mass solubilized in THF.

1.3.2. Size Exclusion Chromatography (SEC)

The evolution of the number-average molecular weight M_n and the weight-average molecular weight M_w were determined using Size Exclusion Chromatography (SEC) experiments. A Dionex Ultimate 3000 liquid chromatograph equipped with one pre-column and two TSK-gel®GMH$_{HR}$-MR columns (7.8 mm ID 30 cm L 5 µm) in series was used, and detection was performed using a refractometer. Chromatogram analyses were performed using PLReanalysis®. The flow rate was fixed at 0.6 mL.min^{-1} using THF as solvent. Low dispersity APS with M_w molar masses ranging from 20 000 to 1 800 000 g.mol^{-1} (Sigma-Aldrich) were used as standards for calibration. All samples analyzed were dissolved in THF at 1 mg.mL^{-1}.

Scission and crosslinking radiation chemical yields, G(S) and G(X), respectively, were calculated using the Charlesby-Pinner (Charlesby and Pinner, 1959) given Equation 3.

$$s + \sqrt{s} = \frac{G(S)}{2 \cdot G(X)} + \frac{9.6 \cdot 10^5}{2 \cdot G(X) \cdot M_{n,0} \cdot D}, \qquad \text{Equation 3}$$

where s is the soluble fraction, D is the dose deposited during the irradiation in Gy, and $M_{n,0}$ is the number-average molecular weight at zero dose in g.mol^{-1}. This equation is based on an initial random distribution of the number-average molecular weight.

1.3.3. Fourier transform infrared spectroscopy (FTIR)

Fourier Transform InfraRed spectra of the polymers were acquired in the reflection mode using a Bruker Vertex 70 spectrometer with a Specac Golden Gate single reflection diamond ATR accessory. The detector used is a DTGS (Deuterated TriGlycine Sulfate), and spectra were acquired in the spectral range between 4 000 and 650 cm^{-1} with a resolution of 2 cm^{-1} and 64 scans to improve the signal-to-noise ratio. Spectra were analyzed with the OMNIC™ software.

2. Results

2.1. Gas release

During the second step of the irradiation, samples of the pre-aged material were irradiated at two different doses: the first at about 0.5 MGy and the second at about 1 MGy. The quantity of gas released was proportional to the dose to ensure the accuracy of the radiation chemical yields. The proposed values in this section are the mean of both values. Figure 1 illustrates the radiation chemical yields of hydrogen release as a function of the dose under the two irradiation atmospheres.

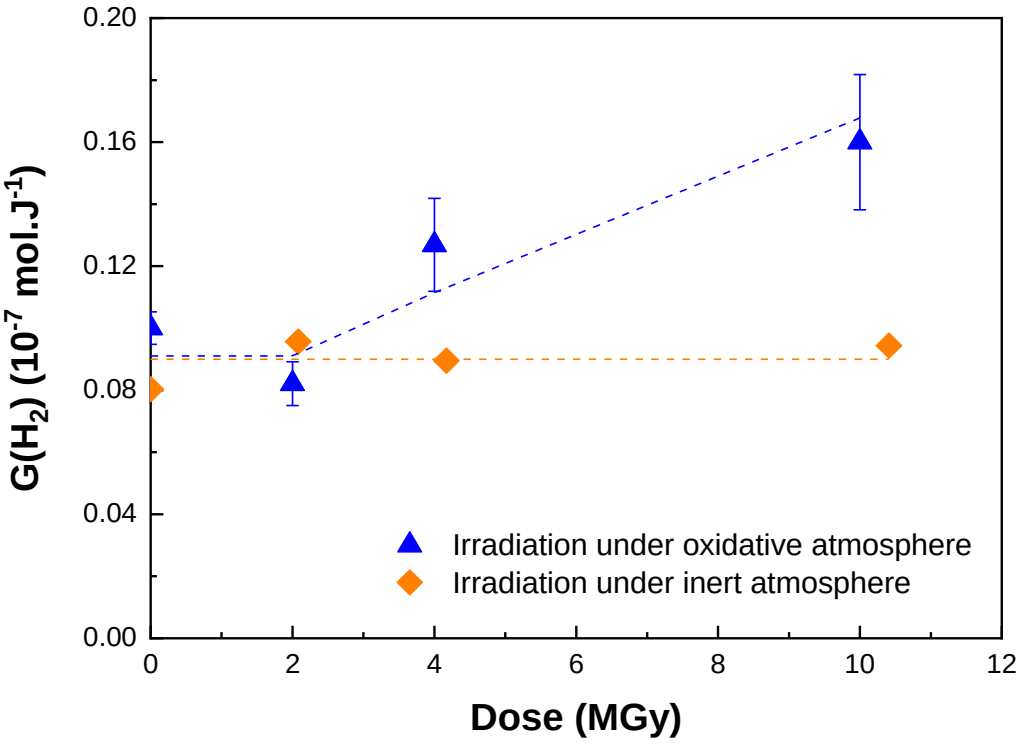

Figure 1. Evolution of $G(H_2)$, the hydrogen radiation chemical yield (in $mol.J^{-1}$) as a function of dose and irradiation atmosphere.

Hydrogen release is found to be very low in APS compared to the one observed in other polyolefins, whatever the irradiation conditions. Hydrogen release radiation chemical yield does not depend on the pre-irradiation dose when irradiation is performed under the inert atmosphere. These results show that even under high LET irradiation and very high doses - more than 10 MGy -the protection conferred by the benzene ring remains efficient. Nevertheless, we have shown that this radiation protection effect proceeds at the expense of the protective group, which is, in this case, the benzene ring (Ferry et al., 2012; Ferry and Ngono, 2021). Figure 1 also shows that, under the oxidative atmosphere, the protective effect of the benzene rings begins to be less effective at doses higher than 2 MGy. At the highest dose, *i.e.,* about 10 MGy, the radiation chemical yield of hydrogen emission under the oxidative atmosphere is twice the value under the inert atmosphere. Thus, under radiation-induced oxidation of APS, the radiation protection conferred by the aromatic ring is reduced after a certain level of modification in the polymer.

Figure 2 shows the evolution of the C_6H_6 emission, quantified in the atmosphere of the ampoules, as a function of the dose. Benzene formation from pristine APS irradiated at 0.5 MGy and 1 MGy is below the quantification limit, but higher doses increase the benzene release radiation chemical

yield. Moreover, in both atmospheres, benzene radiation chemical yield increases linearly with the dose of the first irradiation step. In addition, $G(C_6H_6)$ is higher under the oxidative atmosphere than under the inert atmosphere. This can be related to the fact that one of the polystyrene's weakest points is the tertiary carbon carrying the benzene group, which is highly reactive under oxidation conditions.

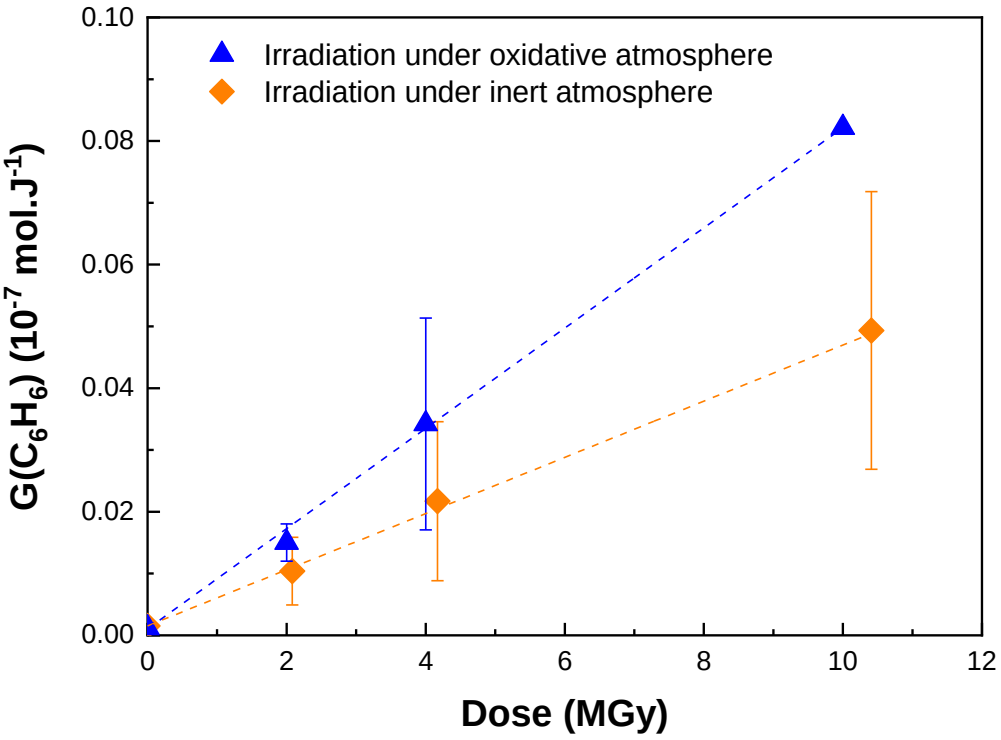

Figure 2. Evolution of $G(C_6H_6)$, the gaseous benzene emission radiation chemical yield (in $mol.J^{-1}$) as a function of dose and the irradiation atmosphere.

Oxygen consumption and carbon oxides release were also quantified (see Figure 3).

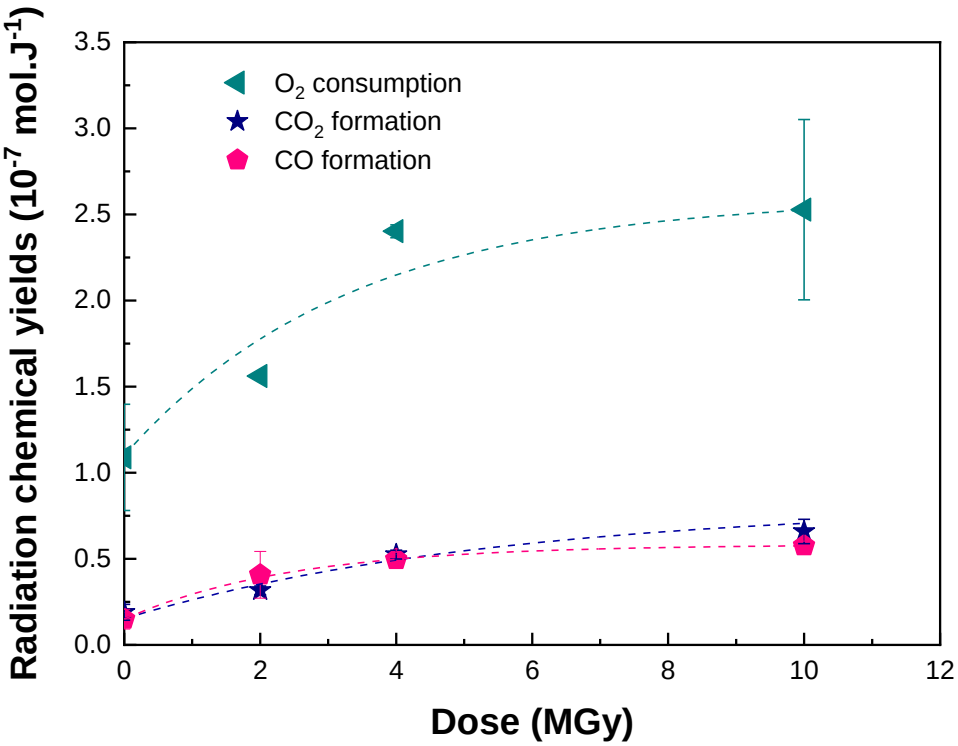

Figure 3. Evolution of the radiation chemical yields of oxygen consumption and carbon oxides releases (in mol.J^{-1}) as a function of dose, in case of irradiation under oxidative conditions.

Contrarily to hydrogen and benzene emissions, oxygen consumption and carbon oxides emission radiation chemical yields tend towards saturation with increasing dose. The equal release of CO and CO_2 aligns with the previous results and with the known radio-oxidation mechanisms. Emission yields of the different gases become roughly constant at doses higher than about 5 MGy. The same behavior holds true for oxygen consumption and is assigned to the partial release of initially consumed oxygen (see the discussion section). Finally, the fact that $\frac{1}{2} \cdot G(CO_2) + G(CO) < G(-O_2)$ demonstrates that part of the incorporated oxygen atoms remains in the polymer backbone.

2.2. Evolution at the macromolecular scale

2.2.1. Soluble fraction

Figure 4 presents the value of the soluble fraction of APS irradiated at different doses, either under inert or oxidative conditions. Error bars correspond to the standard deviation between two measurements in the same conditions. After irradiation, part of the atactic polystyrene becomes

insoluble; the equilibrium content differs from the irradiation conditions. The insoluble fraction reaches an equilibrium roughly equal to 30%$_w$ upon oxidative irradiation at around 5 MGy, whereas APS becomes entirely insoluble under the inert atmosphere from the same dose.

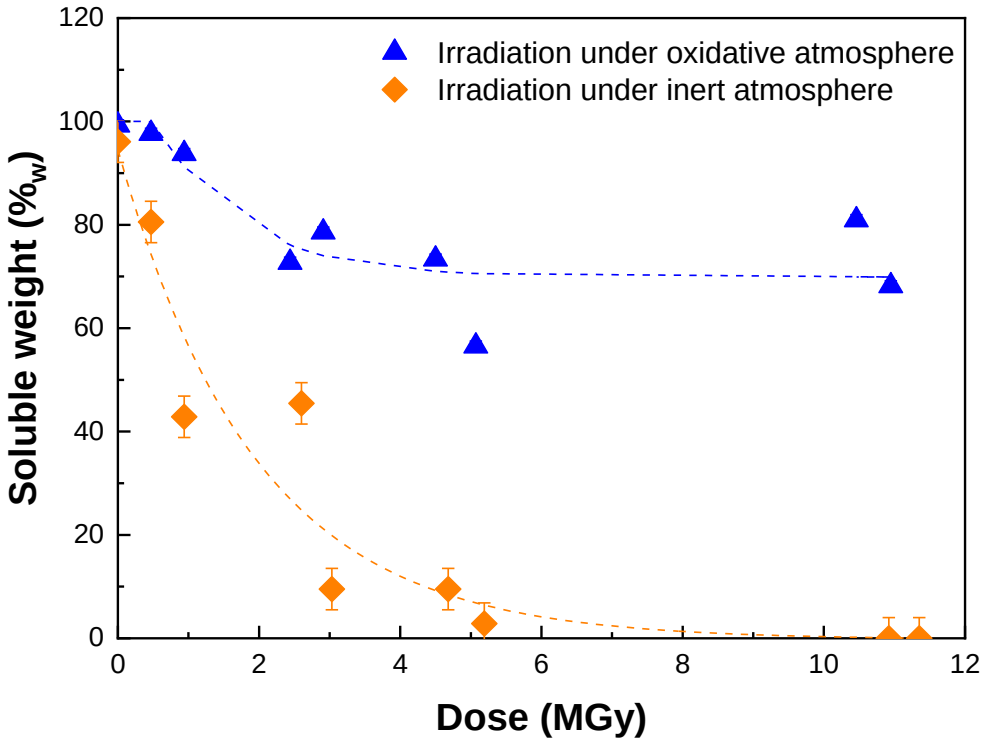

Figure 4. Evolution of the soluble fraction (in %$_w$) as a function of dose and irradiation atmosphere in APS irradiated with SHI.

It is well known that scissions and crosslinking occur simultaneously during irradiation, although with proportions depending on the polymer chemical structure and the irradiation conditions. In the present experimental conditions, crosslinking constitutes the predominant mechanism under the inert atmosphere, whereas chain scissions are no more negligible upon oxidative irradiation and even become preponderant upon crosslinking.

Figure 5 applies the Charlesby-Pinner equation (Charlesby and Pinner, 1959) to the experimental soluble fractions presented in section 2.2.1. Knowing the weight-average molecular weight at zero dose, $M_{w,0}$ (see the following section), the scission and crosslinking radiation chemical yields extrapolated at zero dose were calculated under both irradiation environments:

- Under the inert atmosphere: $G(S) = 0.02 \cdot 10^{-7}$ mol.J^{-1} and $G(X) = 0.05 \cdot 10^{-7}$ mol.J^{-1};
- Under the oxidative atmosphere: $G(S) = 0.09 \cdot 10^{-7}$ mol.J^{-1} and $G(X) = 0.03 \cdot 10^{-7}$ mol.J^{-1}.

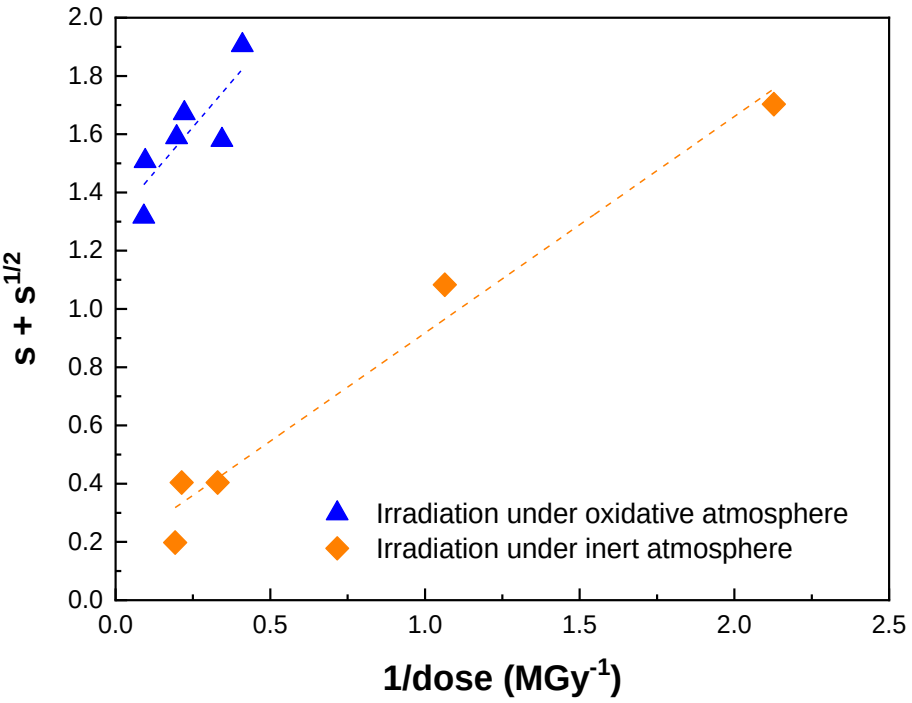

Figure 5. Evolution of the $s+s^{1/2}$ as a function of the inverse of dose. Irradiation under an inert atmosphere and an oxidative atmosphere.

2.2.2. Molecular weights determination

Figure 6 presents the SEC chromatograms of the soluble fraction of irradiated polystyrene samples as a function of the dose and the irradiation atmosphere (irradiation under an inert atmosphere [Figure 6a] and oxidative atmosphere [Figure 6b]).

Under the inert atmosphere, peaks are shifted toward higher elution times when the dose increases, which implies a decrease in the molar mass of the soluble fraction. Moreover, peaks are enlarged only towards the higher elution times, showing that chains are no longer soluble in the solvent once crosslinked. At the highest dose of the present study, SEC peaks almost disappear, indicating the predominance of crosslinking over chain scissions.

Under the oxidative atmosphere, SEC peaks' retention times also increase with increasing doses. Nonetheless, peaks are not as enlarged in the same manner as observed under inert conditions and do not disappear at the highest dose. The peaks' enlargement confirms that the scissions proportion is much more important than the crosslinking one when irradiation is performed under an oxidative atmosphere. Moreover, the peaks' enlargement towards lower elution times indicates that, in these conditions, crosslinking does not necessarily imply polymer insolubilization. Under oxidative atmosphere, two molar mass distributions appear, even at the

lowest doses, in the form of a shoulder at 0.9 MGy and two separated peaks over 2.9 MGy. The appearance of two separate peaks indicates the formation of two populations in terms of molar mass.

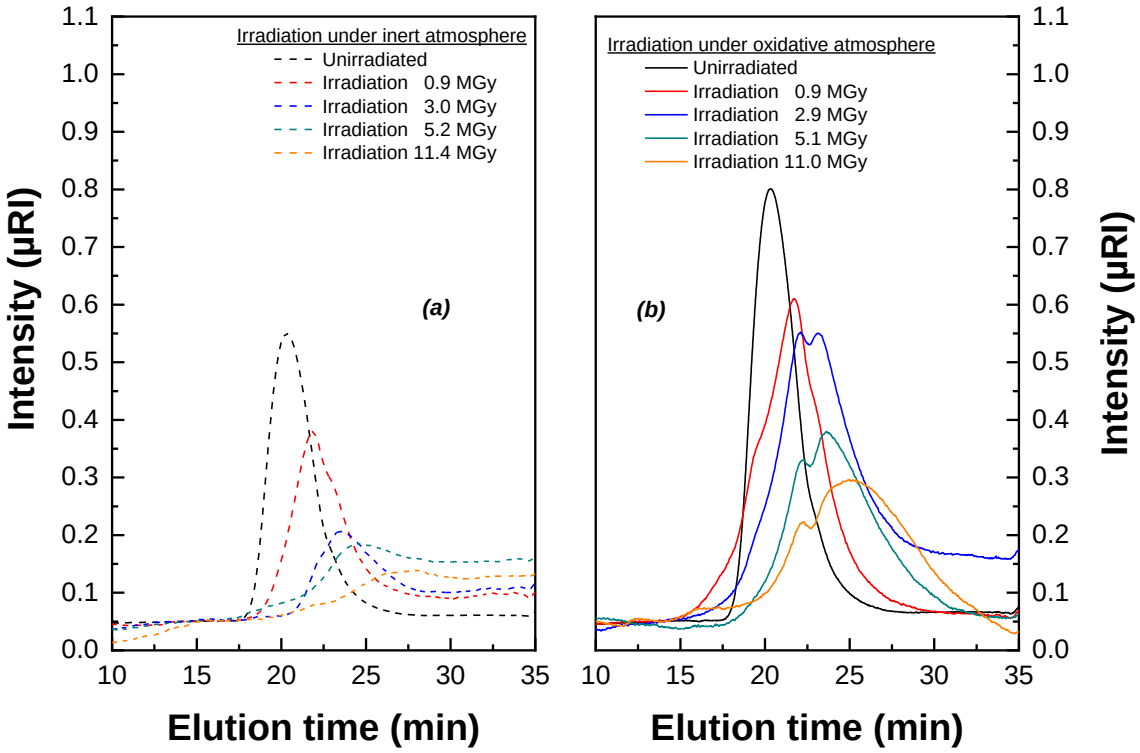

Figure 6. Evolution of the SEC peaks as a function of dose and irradiation atmosphere. (a) Irradiation under an inert atmosphere, (b) irradiation under an oxidative atmosphere.

From the calibration curve, the number-average molar mass (M_n), the weight-average molar mass (M_w), and the dispersity ($Đ$) of the remaining soluble fraction of APS are all determined as a function of the dose and the irradiation atmosphere. Figure 7 shows the average molar mass evolution, and Figure 8 presents the dispersity's evolution as a function of the dose and the irradiation atmosphere.

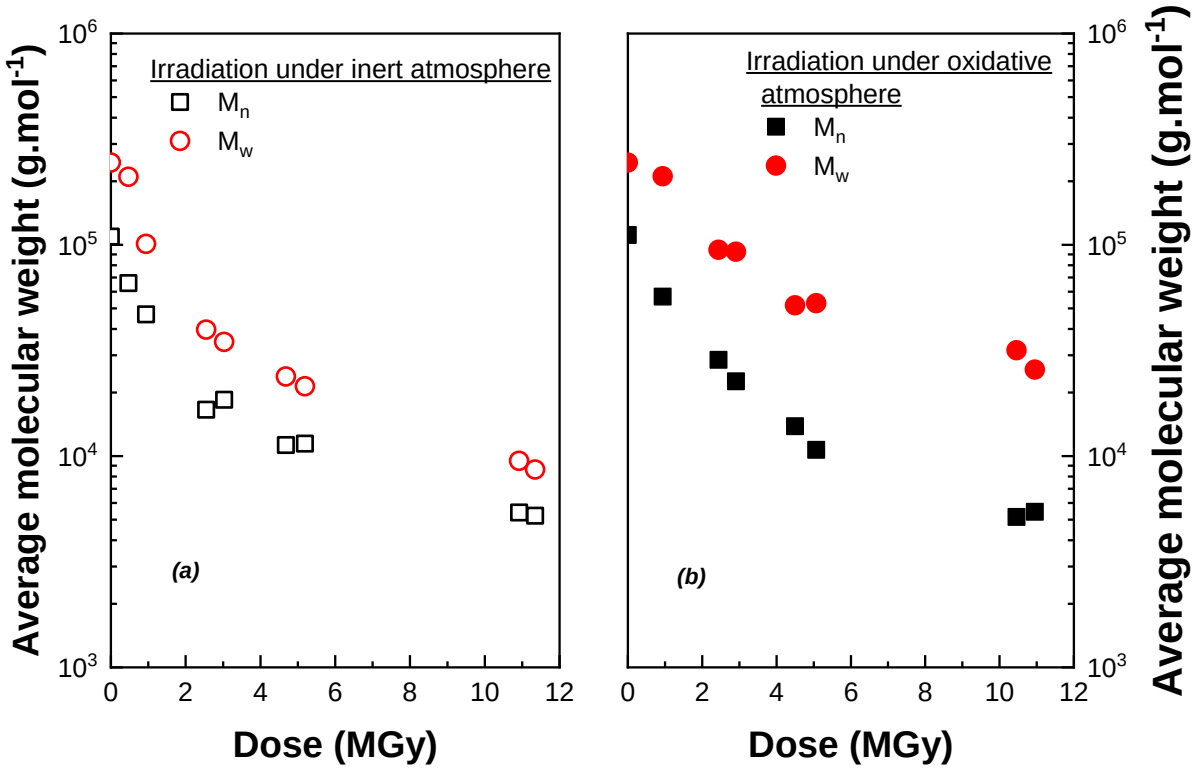

Figure 7. Evolution of the number-average molecular weight M_n and the weight-average molecular weight M_w (in g.mol^{-1}) as a function of dose and irradiation atmosphere in the soluble part. (a) Irradiation under an inert atmosphere, (b) irradiation under an oxidative atmosphere.

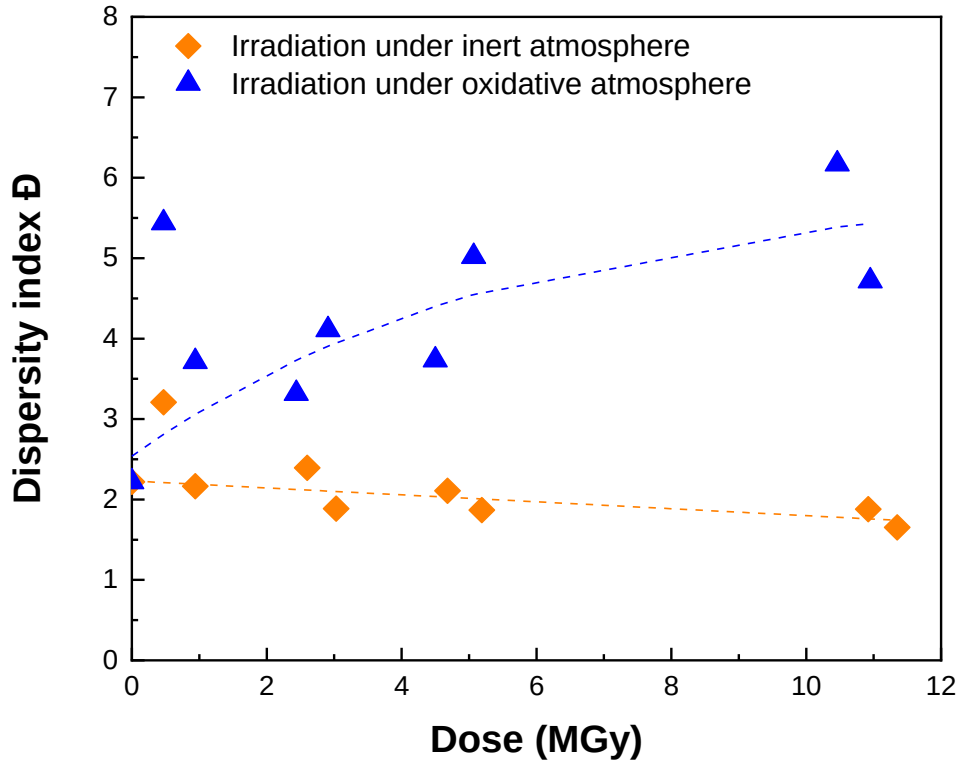

Figure 8. Evolution of the dispersity *Đ* as a function of dose and irradiation atmosphere.

As seen in Figure 7 and as expected, both average molar masses decrease when the dose increases, regardless of the irradiation atmosphere. It can be assumed that higher molar masses are becoming insoluble in almost all cases. Figure 8 shows that dispersity does not follow the same trend as a function of the dose under both atmospheres: whereas dispersity decreases slowly with increasing dose under the inert atmosphere, it increases with increasing dose under the oxidative atmosphere. The behavior under the oxidative atmosphere implies a significant heterogeneity of the average molar masses, *i.e.,* a rather large variety of chain lengths, showing in some way the statistical repartition of the scissions and crosslinking. In contrast, the decrease of *Đ* with increasing dose when irradiation is performed under the inert atmosphere implies a narrowing of the average molar masses distribution, which can be linked to the very low remaining soluble fraction at high doses under this atmosphere, as shown in the previous section in Figure 4.

2.3. Evolution at the molecular scale

Scission to crosslinking ratios provide insights into the polystyrene films' evolution at the macromolecular level when irradiated with SHI.

Ferry *et al.* (Ferry et al., 2008) have already provided modifications induced by SHI under an inert atmosphere. To our knowledge, this is the first study to investigate APS irradiated with SHI under oxidative atmosphere.

Figure 9 presents the FTIR spectra' evolution as a function of the dose. The pristine APS band assignments can be found in Nyquist *et al.* (Nyquist et al., 1992) following the notation of Liang & Krimm (Liang and Krimm, 1958). Three massifs emerge due to molecular modifications by FTIR in polymers irradiated under an oxidative atmosphere: the 3800-3000 cm^{-1} area linked to the υ_{O-H} stretching vibrations (H-bonded or free OH in alcohols and hydroperoxides), the 1850-1550 cm^{-1} area linked to the $\upsilon_{C=O}$ and $\upsilon_{C=C}$ stretching vibrations (esters, ketones, carboxylic acids, and/or C=C double bonds), and the 1450-1050 cm^{-1} area linked to the υ_{C-O} stretching vibrations.

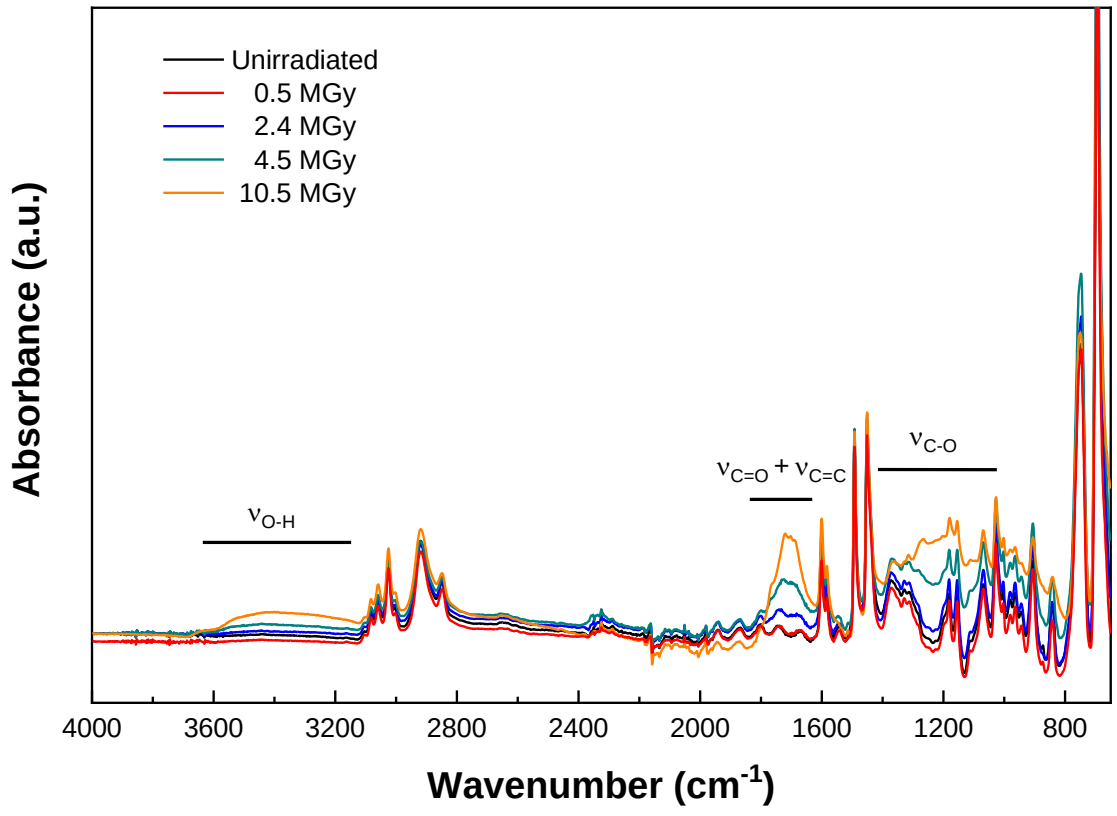

Figure 9. FTIR spectra evolution as a function of dose, for APS irradiated under oxidative conditions.

Two methods can be applied to identify precisely the hidden chemical functions which absorption bands are located under the massifs: chemical derivation and deconvolution. This work in particular analyzes the FTIR spectra using mathematical adjustments. The υ_{O-H} stretching vibration absorption band is highly dependent on H-bond interactions; this dependency induces uncertainties on the exact band position and width. The υ_{C-O} stretching vibration massif is firmly hidden in the pristine polymer characteristic bands and is therefore hardly accessible. In contrast, the $\upsilon_{C=O}$ and $\upsilon_{C=C}$ stretching vibration absorption bands area is relatively well known, not for polystyrene but at least for the most common polymer, *i.e.,* polyethylene.

The 1850-1550 cm^{-1} spectra area is fitted using the band positions given in **Erreur ! Source du renvoi introuvable.**. The spectrum from the irradiated polystyrene film was subtracted by the pristine spectrum by canceling the 1490 cm^{-1} band (representative of the $\nu_{19A}(A_1)$ vibration - an aromatic ring breath), and the chosen baseline was 1877 – 1581 cm^{-1}.

Table 2. FTIR band assignments in the 1820-1550 cm^{-1} area.

Position (cm^{-1})	Attribution	Reference
1785	Perester	(Geuskens et al., 1978a; Mailhot and Gardette, 1992)
1765	Peracid + perester	(Geuskens et al., 1978a)
1732	Aromatic carboxylic acid - associated form	(Mailhot and Gardette, 1992)
1725	Aliphatic ketone	(Geuskens et al., 1978a; Mailhot and Gardette, 1992)
1710	Aliphatic carboxylic acid	(Mailhot and Gardette, 1992)
1704	Aldehyde	(Mailhot and Gardette, 1992)
1700	Aromatic carboxylic acid - dimer	(Mailhot and Gardette, 1992)
1690	Unsaturated or aromatic ketone	(Geuskens et al., 1978a; Mailhot and Gardette, 1992)
1663	In-phase vibration of aliphatic conjugated alkene and/or vinylidene	(Colthup et al., 1990)
1630	Vinyle	(Colthup et al., 1990)
1616	Out-of-phase vibration of aliphatic conjugated alkene	(Colthup et al., 1990)

Figure 10 presents the results obtained as a function of dose: C=C and C=O bonds are formed when APS is irradiated with SHI under the oxidative atmosphere. Both types of bonds do not present any dose threshold before being formed. These defects are the same as those created upon irradiations with low LET irradiations (e.g., γ-rays) under oxidative environments, and these defects are created from the lowest doses. Thus, under SHI, the defects are assumed to be created through the same mechanisms, with very little influence of the high excitation and ionizing density.

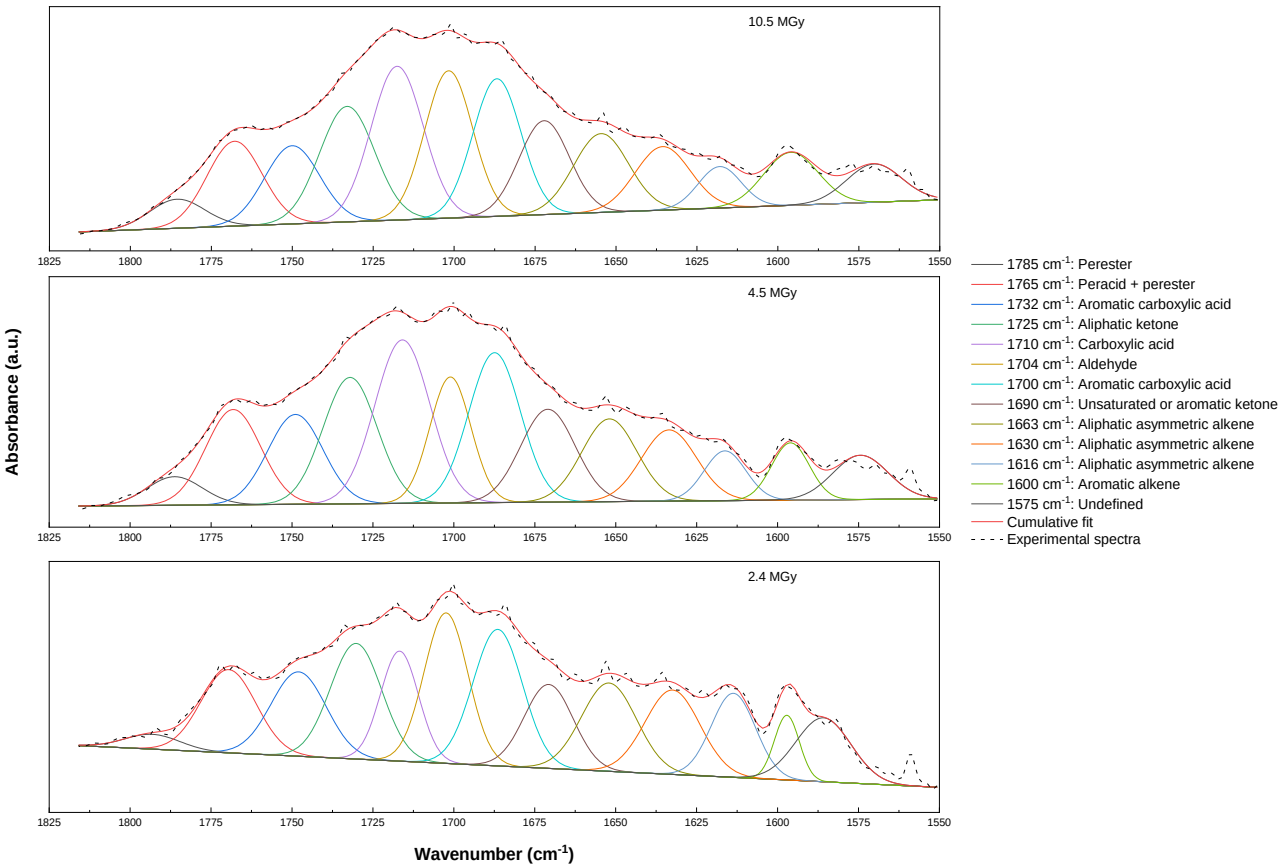

Figure 10. FTIR spectra evolution as a function of dose, in case of irradiation under oxidative conditions, along with the mathematical fit using Origin®. All spectra have been subtracted by the pristine one by cancelling the 1490 cm^{-1} band. Zoom on the 1820-1550 cm^{-1} area.

3. Discussion

Under the inert atmosphere, crosslinking is the predominant ageing process in polystyrene irradiated with SHI beam. Crosslinking allows APS become insoluble from about 5 MGy. **Erreur ! Source du renvoi introuvable.** summarizes the scissions and crosslinking radiation chemical yields for APS, including those from this work and the literature.

Table 3. Scissions and crosslinking radiation chemical yields from the literature and in this work.

	Atmosphere	G(X) (10^{-7} mol.J^{-1})	G(S) (10^{-7} mol.J^{-1})	Reference
γ-rays	Vacuum	0.034±0.002		(Parkinson et al., 1965)
γ-rays	Vacuum	0.037	0.023	(Egusa et al., 1980)
2.5 MeV ^{1}H	Vacuum	0.14		(Bouffard et al., 1997))
118 MeV ^{13}C	Vacuum	0.43		(Bouffard et al., 1997))
3.7 eV/A fast neutrons	Vacuum	0.21±0.09	0.23	(Egusa et al., 1980)
100 keV Ga	Vacuum	0.093		(Seki et al., 2004)
MeV order ion beam	Vacuum	1.9		(Seki et al., 2004)
89 MeV/A ^{36}Ar	Inert atmosphere	0.05	0.02	This work
γ-rays	Air	0.037	0.16	(Egusa et al., 1980)
γ-rays (at the surface of the thick film)	Air	0.026	0.10	(Bowmer et al., 1979)
3.7 eV/A fast neutrons	Air	0.07±0.03	0.11	(Egusa et al., 1980)
89 MeV/A ^{36}Ar	Oxidative atmosphere	0.03	0.09	This work

Using the Charlesby-Pinner equation (Equation 3), the G(X) values obtained in this work from experiments under an inert atmosphere lie between those obtained under γ-rays and those from the literature obtained using SHI, excepting the values from the work of Seki *et al.* (Seki et al., 2004). As LET in this study (2.5 MeV.mg^{-1}.cm^{-2}) is higher than those in the work of Bouffard *et al.* (Bouffard et al., 1997)(about 0.19 MeV.mg^{-1}.cm^{-2} for 2.5 MeV ^{1}H and 1.8 MeV.mg^{-1}.cm^{-2} for 118 MeV ^{13}C), a higher crosslinking radiation chemical yield was expected in the present work. The discrepancy likely comes from the differences in the initial molecular weights of the polymer employed: $M_{w,0}$ is more than 20 times higher in this work than in the one of Bouffard *et al.* (Bouffard et al., 1997). This hypothesis seems confirmed by the observations of Egusa *et al.* (Egusa et al., 1980), who demonstrated that the increase of the chain length induces a decrease of G(X) when irradiation is performed using fast neutrons. The present work shows that crosslinking is

predominant over scission under an inert atmosphere, which aligns with results from the literature (Audouin et al., 2012; Ferry et al., 2016a; Grassie and Weir, 1965a; Kiryukhin, 1989; Puglisi et al., 1986). There are more uncertainties on the scission potentiality. Calcagno *et al.* (Calcagno et al., 1992) indicate that there are no scission in APS irradiated under an inert atmosphere. In contrast, we evidenced scissions, even if their radiation chemical yields are almost four times lower than those of crosslinkings.

Hydrogen and benzene emissions were observed using gas mass spectrometry. Previous work (Ferry et al., 2008) has already shown that significant formation of mono- or disubstituted cyclohexadienes does not occur. Thus, the Puglisi *et al.* (Puglisi et al., 1986) mechanism, which establishes crosslinking through cyclohexadiene bridges with no hydrogen emission, is neither the only nor the predominant mechanism leading to crosslinking. According to Dole (Dole, 1972), crosslinking follows the same evolution as hydrogen emission, leading to the hypothesis that they are formed from a common mechanism. As we did not observe the same evolution in the present experiments, this hypothesis is excluded here, at least as the sole mechanism leading to H_2. The production of hydrogen from more than one reaction mechanism is highly probable. Ferry *et al.* (Ferry et al., 2008) observed that double bonds formation as a function of the dose would follow the same evolution as benzene. The fact that $G(H_2)$ and $G(C_6H_6)$ do not present the same evolution with the dose indicates that these two molecules are not formed within the same reaction mechanism.

Taking into account all the new bonds that have been identified in this work, hypotheses on some of the reaction mechanisms leading to these products can be performed. Non exhaustively, possible reaction pathways are summarized in Scheme 1.

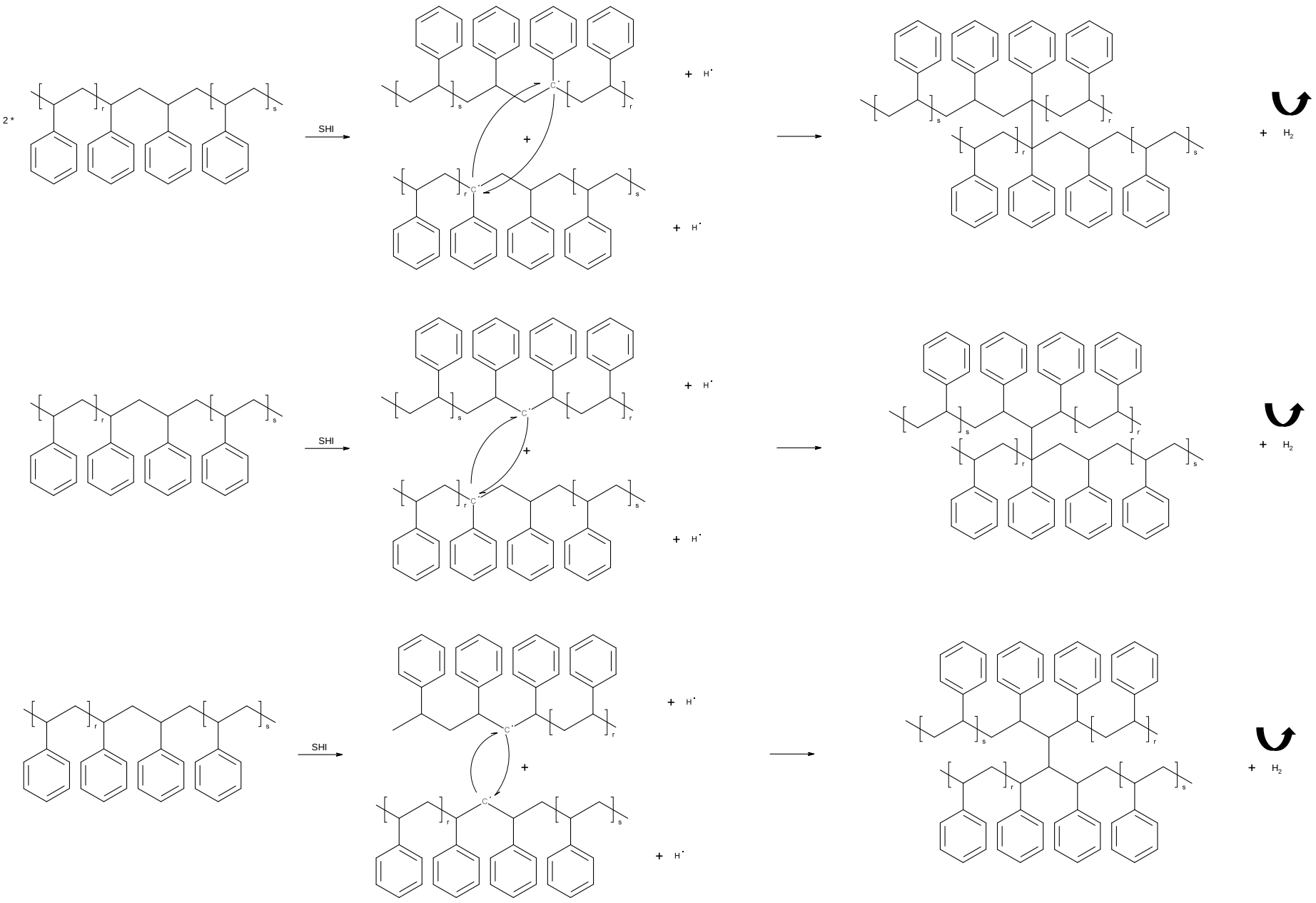
2 *
SHI
+ H·
+ H·
+ H2
SHI
+ H·
+ H·
+ H2
SHI
+ H·
+ H·
+ H2

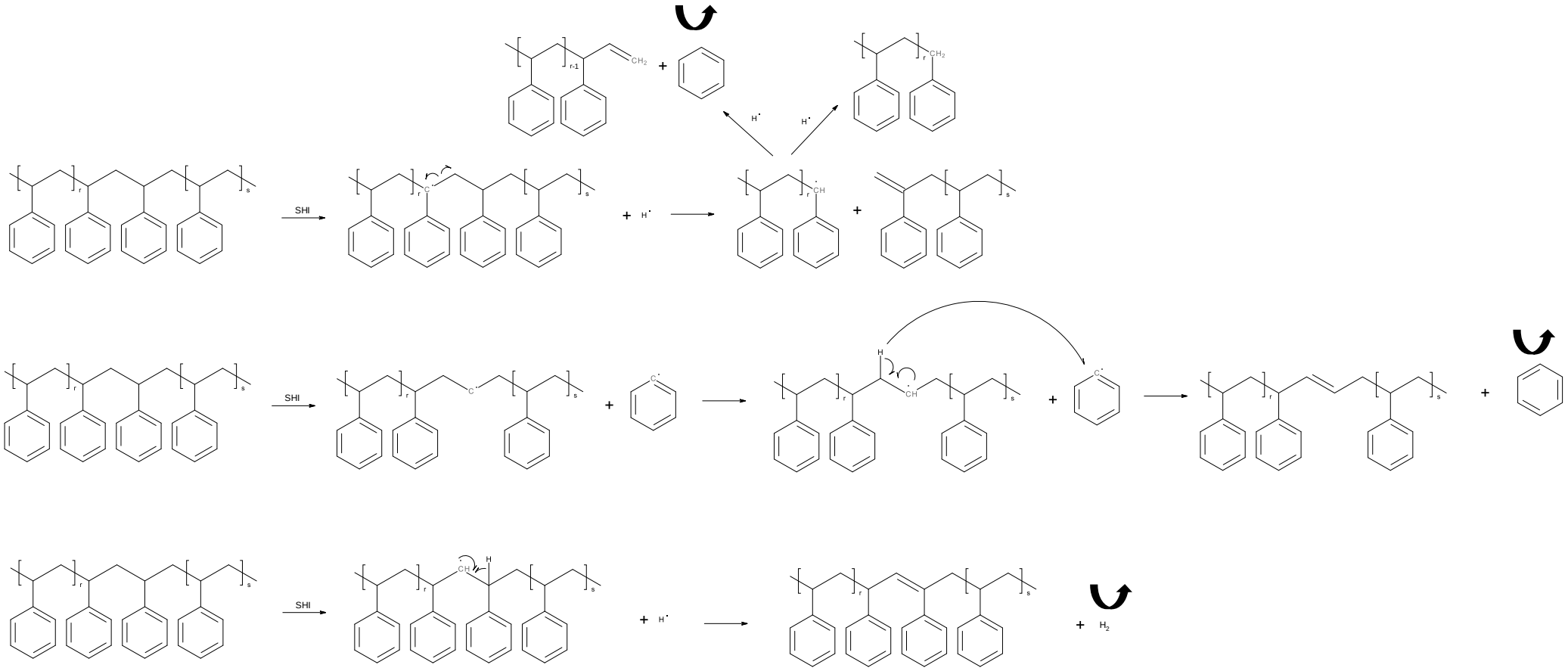

Scheme 1. Possible reaction mechanisms under an inert atmosphere.

Studies of polystyrene aged under an oxidative atmosphere are scarce in the literature, and most of them concern studies under photo-oxidation at 253.7 nm (Geuskens et al., 1978a; Geuskens et al., 1978b; Grassie and Weir, 1965a, b). In such conditions, which are very different from the conditions used in the present work, crosslinking remains the main process, even under oxygen.

Erreur ! Source du renvoi introuvable. shows that the G(X) and G(S) values of this work are not so far from the literature obtained in APS irradiated with γ-rays under an oxidative atmosphere (Bowmer et al., 1979; Egusa et al., 1980). The ratios $G_{inert}/G_{oxidative\ atmosphere}$ in our work and the work of Egusa *et al.* (Egusa et al., 1980) do not follow perfectly the same trend. According to these authors, G(X) is divided by a factor 3 and G(S) by a factor 2 when irradiations are performed with fast neutrons under air as compared to irradiations under vacuum. To the best of our knowledge, this slight discrepancy between our results and those from the literature comes from differences in the energy deposition structure between SHI irradiations and fast neutrons.

Bowmer *et al.* (Bowmer et al., 1979) found that $G(S)/G(X) = 3.7$ in conditions of homogeneous oxidation (powder) and 1.0 in conditions of heterogeneous oxidation conditions (sheats). Later, Egusa *et al.* (Egusa et al., 1980) found that $G(S)/G(X) \approx 4.5$, when irradiations were under homogeneous oxidation conditions. This study found that $G(S)/G(X) = 2.6$, below the two earlier values. This difference is explained by the heterogeneous energy deposition pattern of ion beams, which has been proven under an inert atmosphere (Gervais and Bouffard, 1994) and under an oxidative atmosphere (Gervais et al., 2021). In the conditions employed in this study, APS is irradiated under homogenous conditions of oxidation. However, under high LET irradiation, radicals are formed in ion tracks where their concentration is high enough to allow part of them to react with each other before reacting with oxygen (Waligórski et al., 1986).

The generally used yet outdated Bolland and Gee mechanism (Bolland and Gee, 1946) is given in Scheme 2. In the case of low LET irradiations under homogeneous oxidation conditions, reaction 6 is predominant over reaction 4 and reaction 5. By contrast, even in homogeneous oxidation conditions, reaction 4 and/or reaction 5 are no longer negligible under SHI irradiations.

$PH \xrightarrow{Irradiation} P° + H°$	Initiation
$P° + O_2 \rightarrow POO°$	First step of propagation
$POO° + PH \rightarrow POOH + P°$	Second step of propagation
$P° + P° \rightarrow P\text{-}P$	Termination - Reaction 4
$POO° + P° \rightarrow$ inactive products	Termination - Reaction 5
$POO° + POO° \rightarrow$ inactive products	Termination - Reaction 6

Scheme 2. Bolland and Gee mechanism (Bolland and Gee, 1946). PH represents the polymer, P° the alkyl radical, POO° the peroxide radical and POOH the hydroperoxide.

Under the oxidative atmosphere, benzene release is twice as much as under the inert atmosphere. This result can be explained by part of the reaction mechanisms given in Scheme 3, which is a common evn though partial reaction pathway when irradiations are performed under an oxidative atmosphere. This result also implies the formation of peroxide radicals (first step of propagation in Scheme 2), reacting together to form alkoxy radicals (PO°) and then stabilizing themselves as aliphatic ketones (as evidenced by FTIR spectroscopy and shown in Figure 10) by releasing a benzene molecule through β-scission. This reaction occurs alongside the benzene release mechanism proposed under an inert atmosphere (Scheme 1) and explains the higher benzene radiation chemical yield observed under the oxidative atmosphere.

Under the oxidative atmosphere, hydrogen emission yield was roughly constant and equivalent to the yield determined under the inert atmosphere up to about 2 MGy; the yield then increased for higher doses. At the highest dose of this study, $G(H_2)$ was doubled under the oxidative atmosphere just like $G(C_6H_6)$ under the same conditions.

FTIR spectroscopy shows that various oxidized defects are formed upon irradiation: -OH, C=O and C-O massifs are easily visible on the spectra. Thanks to the mathematical adjustment in the 1660 – 1600 cm^{-1} area, it has also been determined that double bonds of the C=C type are formed. These bands are expected because of the intra-tracks recombination of non-oxidized radicals, even though the sample thickness is inferior to the critical thickness of oxidation (Ngono-Ravache et al., 2015). Surprisingly, the same massif/evolution can be found when polystyrene is photo-oxidized (Mailhot and Gardette, 1992). This observation might suggest that the benzene rings react to form another type of asymmetric C=C double bond, e.g., by ring opening. Although the irradiation conditions in Mailhot and Gardette's study are quite different from ours, the formation of most of the defects identified by FTIR in the C=O double bonds massif can be explained for many of the common radio-oxidation mechanisms.

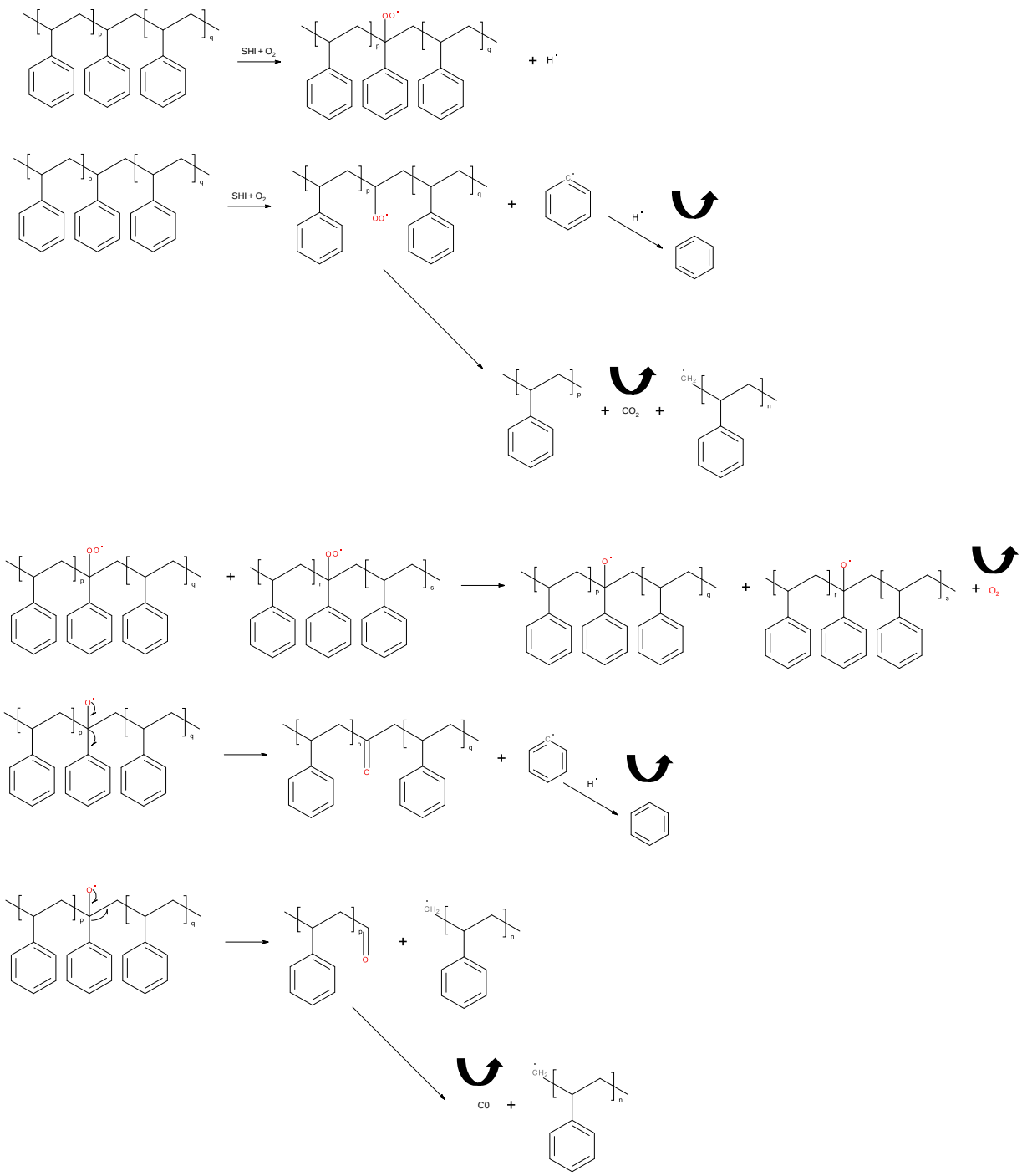

Scheme 3. Possible reaction mechanisms under an oxidative atmosphere.

The main difference between APS irradiation with SHI under the inert and under the oxidative atmosphere is the reduced radiation protection conferred by the benzene ring when oxygen is present. The two markers of this impairment in the radiation protection are related to the hydrogen and benzene release evolution that occurs with increasing dose. The first marker is visible after a threshold of about 2 MGy, when the hydrogen emission begins to increase. The

second marker occurs when benzene release is doubled in the presence of oxygen compared to inert atmosphere, whatever the dose.

The enhanced scission mechanism is also a cause for the accelerated ageing under oxygen compared to irradiation under inert atmosphere. However, within the large dose range studied in this work, the degradation observed in APS remains low in all cases: although a cumulative effect is observed in the formation of new bonds, their concentrations are moderated, especially when compared to polyolefins (Ferry et al., 2016b; Ngono-Ravache et al., 2015).

Conclusion

Modifications induced in polystyrene by SHI irradiation are studied by analyzing oxygen consumption, gas release, macromolecular (scission, crosslinking, gel fraction, average molecular weights evolutions), and molecular (FTIR spectroscopy) levels.

Comparisons between SHI irradiation-induced ageing of atactic polystyrene under the inert and the oxidative atmospheres in conditions of homogenous oxidation are evaluated up to doses as high as 10 MGy. Some of the mechanisms of atactic polystyrene ageing proposed in the literature are reevaluated, and the most probable ones are discussed. Under homogenous oxidation conditions, a material that would stay completely soluble is expected; however, due to the SHI irradiation dose deposition specificity, part of the radicals recombine instead of reacting with oxygen. This structure leads to crosslinking in the ion tracks and ultimately to the decrease of the soluble fraction, even under the oxidative atmosphere. C=C double bonds and the more expected carbonyl bonds were also observed.

Hydrogen and benzene releases tend to increase under the oxidative atmosphere, showing the lowering of the aromatic rings radiation protection efficiency. Nonetheless, the H_2 radiation chemical yield remains at least 20 times lower than that of polyethylene, even at doses as high as 10 MGy. Relatedly benzene release is more important under the oxygen atmosphere but is still limited. Finally, oxygen consumption and release of carbon oxides are markedly lower than those observed when studying polyethylene.

This study is the first evaluation of the dose and atmosphere effects on one of the most stable polymers. Our work offers the first insights into the stability of polymers when increasing the complexity of irradiation. Benzene and polystyrene are known to lose their stability when LET increases. In the conditions of this study, *i.e.,* at a LET roughly equal to the one of α emitters, stability remains effective even at high doses and under an oxidative atmosphere. However, this protection is at the expense of the aromatic ring released in the surrounding atmosphere.

Acknowledgments

Orano, EDF, and CEA funded this study as part of the CEA COSTO project. The authors would like to thank Vincent Dauvois (CEA/SPC) for his help during the high-resolution gas mass analyses and Marie-Claude Clochard (CEA/LSI) for supplying APS standards with a low dispersity for SEC calibration.

References

Alexander, P., Toms, D., 1956. The effect of oxygen on the changes produced by ionizing radiations in polymers. Journal of Polymer Science 22, 343-348.
Audouin, L., Colin, X., Fayolle, B., Richaud, E., Verdu, J., 2012. Polymères en ambiance nucléaire. Comportement à long terme, Les Ulis, France.
Balanzat, E., Bouffard, S., Bouquerel, A., Devy, J., Gaté, C., 1996. Swift heavy ion irradiation of polystyrene. Nuclear Instruments and Methods in Physics Research Section B: Beam Interactions with Materials and Atoms 116, 159-163.
Bolland, J.L., Gee, G., 1946. Kinetic studies in the chemistry of rubber and related materials. II. The kinetics of oxidation of unconjugated olefins. Transactions of the Faraday Society 42, 236-243.
Bouffard, S., Balanzat, E., Leroy, C., Busnel, J.P., Guevelou, G., 1997. Cross-links induced by swift heavy ion irradiation in polystyrene. Nuclear Instruments and Methods in Physics Research Section B: Beam Interactions with Materials and Atoms 131, 79-84.
Boughattas, I., Ferry, M., Dauvois, V., Lamouroux, C., Dannoux-Papin, A., Leoni, E., Balanzat, E., Esnouf, S., 2016. Thermal degradation of γ-irradiated PVC: I-dynamical experiments. Polymer Degradation and Stability 126, 219-226.
Bowmer, T.N., Cowen, L.K., O'Donnell, J.H., Winzor, D.J., 1979. Degradation of polystyrene by gamma irradiation: Effect of air on the radiation-induced changes in mechanical and molecular properties. Journal of Applied Polymer Science 24, 425-439.
Calcagno, L., Compagnini, G., Foti, G., 1992. Structural modification of polymer films by ion irradiation. Nuclear Instruments and Methods in Physics Research Section B: Beam Interactions with Materials and Atoms 65, IN7-422.
Chang, Z., LaVerne, J.A., 2000. Hydrogen Production in the Heavy Ion Radiolysis of Polymers. 1. Polyethylene, Polypropylene, Poly(methyl methacrylate), and Polystyrene. Journal Physical Chemistry B 104, 10557.
Charlesby, A., Pinner, S.H., 1959. Analysis of the solubility behaviour of irradiated polyethylene and other polymers. Proceedings of the Royal Society of London. Series A. Mathematical and Physical Sciences 249, 367-386.
Choi, S.C., Han, S., Choi, W.K., Jung, H.J., Koh, S.K., 1999. Hydrophilic group formation on hydrocarbon polypropylene and polystyrene by ion-assisted reaction in an O2 environment. Nuclear Instruments and Methods in Physics Research Section B: Beam Interactions with Materials and Atoms 152, 291-300.
Colthup, N.B., Daly, L.H., Wiberley, S.E., 1990. Introduction to Infrared and Raman Spectroscopy - 3rd Edition, Third Edition ed. Academic Press, Inc., Boston.
Dole, M., 1972. The Radiation Chemistry of Macromolecules. Academic Press.
Egusa, S., Ishigure, K., Tabata, Y., 1980. Fast Neutron Irradiation Effects on Polymers. 2. Cross-Linking and Degradation of Polystyrene. Macromolecules 13, 171-176.
Ferry, M., Bessy, E., Harris, H., Lutz, P.J., Ramillon, J.M., Ngono-Ravache, Y., Balanzat, E., 2012. Irradiation of Ethylene/Styrene Copolymers: Evidence of Sensitization of the Aromatic Moiety As Counterpart of the Radiation Protection Effect. The Journal of Physical Chemistry B 116, 1772.
Ferry, M., Carpentier, F., Cornaton, M., 2021a. Radio-Oxidation Ageing of XLPE Containing Different Additives and Filler: Effect on the Gases Emission and Consumption. Polymers 13, 2845.

Ferry, M., Dannoux-Papin, A., Dély, N., Legand, S., Durand, D., Roujou, J.L., Lamouroux, C., Dauvois, V., Coignet, P., Cochin, F., Esnouf, S., 2014. Chemical composition effects of methylene containing polymers on gas emission under γ-irradiation. Nuclear Instruments and Methods in Physics Research Section B: Beam Interactions with Materials and Atoms 334, 69-76.
Ferry, M., Esnouf, S., Leprêtre, F., Cabet, C., Bender, M., Severin, D., Balanzat, E., Ngono, Y., 2021b. Effect of oxygen on gas emitted from polymer irradiated using Swift Heavy Ion beams. Nuclear Instruments and Methods in Physics Research Section B: Beam Interactions with Materials and Atoms 497, 51-58.
Ferry, M., Ngono-Ravache, Y., Aymes-Chodur, C., Clochard, M.C., Coqueret, X., Cortella, L., Pellizzi, E., Rouif, S., Esnouf, S., 2016a. Ionizing Radiation Effects in Polymers, Reference Module in Materials Science and Materials Engineering. Elsevier.
Ferry, M., Ngono-Ravache, Y., Picq, V., Balanzat, E., 2008. Irradiation of Atactic Polystyrene: Linear Energy Transfer Effects. Journal of Physical Chemistry B 112, 10879.
Ferry, M., Ngono, Y., 2021. Energy transfer in polymers submitted to ionizing radiation: A review. Radiation Physics and Chemistry 180, 109320.
Ferry, M., Pellizzi, E., Boughattas, I., Fromentin, E., Dauvois, V., de Combarieu, G., Coignet, P., Cochin, F., Ngono-Ravache, Y., Balanzat, E., Esnouf, S., 2016b. Effect of cumulated dose on hydrogen emission from polyethylene irradiated under oxidative atmosphere using gamma rays and ion beams. Radiation Physics and Chemistry 118, 124-127.
Fromentin, E., Aymes-Chodur, C., Doizi, D., Cornaton, M., Miserque, F., Cochin, F., Ferry, M., 2017. On the radio-oxidation, at high doses, of an industrial polyesterurethane and its pure resin. Polymer Degradation and Stability 146, 161-173.
Furtak-Wrona, K., Cornaton, M., Durand, D., Dauvois, V., Roujou, J.L., Esnouf, S., Ferry, M., 2019. Temperature and LET effects on radiation-induced modifications in non-perfect polyethylenes. Polymer Degradation and Stability 162, 66-75.
Gervais, B., Bouffard, S., 1994. Simulation of the primary stage of the interaction of swift heavy ions with condensed matter. Nuclear Instruments and Methods in Physics Research Section B: Beam Interactions with Materials and Atoms 88, 355-364.
Gervais, B., Ngono, Y., Balanzat, E., 2021. Kinetic Monte Carlo simulation of heterogeneous and homogeneous radio-oxidation of a polymer. Polymer Degradation and Stability 185, 109493.
Geuskens, G., Baeyens-Volant, D., Delaunois, G., Lu-Vinh, Q., Piret, W., David, C., 1978a. Photo-oxidation of polymers—I: A quantitative study of the chemical reactions resulting from irradiation of polystyrene at 253.7 nm in the presence of oxygen. European Polymer Journal 14, 291-297.
Geuskens, G., Baeyens-Volant, D., Delaunois, G., Lu Vinh, Q., Piret, W., David, C., 1978b. Photo-oxidation of polymers—II: The sensitized decomposition of hydroperoxides as the main path for initiation of the photo-oxidation of polystyrene irradiated at 253.7 nm. European Polymer Journal 14, 299-303.
Gillen, K., Clough, R., 1991. Accelerated aging methods for predicting long-term mechanical performance of polymers, Irradiation effects on polymers. Elsevier Applied Science, London, pp. 157-223.
Grassie, N., Weir, N.A., 1965a. The photooxidation of polymers. II. Photolysis of polystyrene. Journal of Applied Polymer Science 9, 975-986.
Grassie, N., Weir, N.A., 1965b. The photooxidation of polymers. III. Photooxidation of polystyrene. Journal of Applied Polymer Science 9, 987-998.
Hettal, S., Suraci, S.V., Roland, S., Fabiani, D., Colin, X., 2021. Towards a Kinetic Modeling of the Changes in the Electrical Properties of Cable Insulation during Radio-Thermal Ageing in Nuclear Power Plants. Application to Silane-Crosslinked Polyethylene. Polymers 13, 4427.
Kiryukhin, V.P., 1989. Radiation crosslinking and chain scission of polymers, in: Milinchuk, V.K., Tupikov, V.I. (Eds.), Organic radiation chemistry handbook. Ellis Horwood Limited, Chichester.
Klaumünzer, S., Zhu, Q.Q., Schnabel, W., Schumacher, G., 1996. Ion-beam-induced crosslinking of polystyrene — still an unsolved puzzle. Nuclear Instruments and Methods in Physics Research Section B: Beam Interactions with Materials and Atoms 116, 154-158.
Lewis, M.B., Lee, E.H., 1993. G-values for gas production from ion-irradiated polystyrene. Journal of Nuclear Materials 203, 224-232.

Liang, C.Y., Krimm, S., 1958. Infrared spectra of high polymers. VI. Polystyrene. Journal of Polymer Science 27, 241-254.
Mailhot, B., Gardette, J.L., 1992. Polystyrene photooxidation. 2. A pseudo wavelength effect. Macromolecules 25, 4127-4133.
Ngono-Ravache, Y., Damaj, Z., Dannoux-Papin, A., Ferry, M., Esnouf, S., Cochin, F., De Combarieu, G., Balanzat, E., 2015. Effect of swift heavy ions on an EPDM elastomer in the presence of oxygen: LET effect on the radiation-induced chemical ageing. Polymer Degradation and Stability 111, 89-101.
Nyquist, R.A., Putzig, C.L., Leugers, M.A., McLachlan, R.D., Thill, B., 1992. Comparison of the Vibrational Spectra and Assignments for α-Syndiotactic, β-Syndiotactic, Isotactic, and Atactic Polystyrene and Toluene. Appl. Spectrosc. 46, 981-987.
Parkinson, W.W., Bopp, C.D., Binder, D., White, J.E., 1965. A Comparison of Fast Neutron and γ-Irradiation of Polystyrene. I. Cross-Linking Rates1. The Journal of Physical Chemistry 69, 828-833.
Puglisi, O., Licciardello, A., Pignataro, S., Calcagno, L., Foti, G., 1986. Primary chemical events in ion bombarded polystyrene films: An infrared study. Radiation Effects 98, 161-170.
Seki, S., Tsukuda, S., Maeda, K., Matsui, Y., Saeki, A., Tagawa, S., 2004. Inhomogeneous distribution of crosslinks in ion tracks in polystyrene and polysilanes. Physical Review B 70, 144203.
Skidmore, E., 2012. Review of the aging data on EPDM O-rings in the H1616 shipping package, Report SRNL-STI-2012-00149. Savannah River National Laboratory.
Waligórski, M.P.R., Hamm, R.N., Katz, R., 1986. The radial distribution of dose around the path of a heavy ion in liquid water. International Journal of Radiation Applications and Instrumentation. Part D. Nuclear Tracks and Radiation Measurements 11, 309-319.
Xu, A., Roland, S., Colin, X., 2021. Physico-chemical analysis of a silane-grafted polyethylene stabilised with an excess of Irganox 1076®. Proposal of a microstructural model. Polymer Degradation and Stability 183, 109453.
Ziegler, J.F., Ziegler, M.D., Biersack, J.P., 2010. SRIM – The stopping and range of ions in matter (2010). Nuclear Instruments and Methods in Physics Research Section B: Beam Interactions with Materials and Atoms 268, 1818-1823.